C-terminal 15 kDa fragment of cytoskeletal actin is posttranslationally *N*-myristoylated upon caspase-mediated cleavage and targeted to mitochondria

Toshihiko Utsumi*, Nagisa Sakurai, Kengo Nakano, Rumi Ishisaka

Department of Biological Chemistry, Faculty of Agriculture, Yamaguchi University, Yamaguchi 753-8515, Japan

Received 18 January 2003; revised 14 February 2003; accepted 14 February 2003

First published online 5 March 2003

Edited by Barry Halliwell

Abstract To detect the posttranslational *N*-myristoylation of caspase substrates, the susceptibility of the newly exposed N-terminus of known caspase substrates to protein *N*-myristoylation was evaluated by in vivo metabolic labeling with [^{3}H]myristic acid in transfected cells using a fusion protein in which the query sequence was fused to a model protein. As a result, it was found that the N-terminal nine residues of the newly exposed N-terminus of the caspase-cleavage product of cytoskeletal actin efficiently direct the protein *N*-myristoylation. Metabolic labeling of COS-1 cells transiently transfected with cDNA coding for full-length truncated actin (tActin) revealed the efficient incorporation of [^{3}H]myristic acid into this molecule. When COS-1 cells transiently transfected with cDNA coding for full-length actin were treated with staurosporine, an apoptosis-inducing agent, an *N*-myristoylated tActin was generated. Immunofluorescence staining coupled with MitoTracker or fluorescence tagged-phalloidin staining revealed that exogenously expressed tActin colocalized with mitochondria without affecting cellular and actin morphology. Taken together, these results demonstrate that the C-terminal 15 kDa fragment of cytoskeletal actin is posttranslationally *N*-myristoylated upon caspase-mediated cleavage during apoptosis and targeted to mitochondria.

Key words: Posttranslational modification; Posttranslational *N*-myristoylation; Caspase substrate; Protein *N*-myristoylation; Protein acylation; Actin

1. Introduction

A number of eukaryotic cellular proteins are found to be covalently modified with the 14-carbon saturated fatty acid, myristic acid [1–6]. Many of the myristoylated proteins play key roles in regulating cellular structure and function. They include proteins involved in a wide variety of cellular signal transduction pathways. In general, protein *N*-myristoylation is the result of cotranslational addition of myristic acid to a Gly residue at the extreme N-terminus after removal of the initiating Met by cellular methionylaminopeptidases. A stable amide bond links myristic acid irreversibly to proteins. Recently, it was demonstrated that protein *N*-myristoylation can also occur posttranslationally, as in the case of the pro-apoptotic protein BID where proteolytic cleavage by caspase 8 reveals a 'hidden' myristoylation motif [7]. The posttranslational *N*-myristoylation of BID was demonstrated to be catalyzed by *N*-myristoyltransferase (NMT), the enzyme responsible for cotranslational *N*-myristoylation. It was also revealed that *N*-myristoylation has a strong influence on BID targeting to mitochondria, its insertion into the outer membrane of mitochondria, the release of cytochrome c, and the killing of cells. Thus, posttranslational *N*-myristoylation plays a critical role in the biological activity of BID. Since about one-fourth (16 of ~60) of the identified caspase substrates expose an N-terminal Gly upon cleavage [8], it was suggested that this modification might be a common posttranslational modification in the apoptosis pathway [7]. However, so far, BID is the only protein that has been proved experimentally to be posttranslationally *N*-myristoylated upon cleavage by caspase. One possible reason for this might be the lack of a convenient method to detect this unusual modification. In a previous study, we have shown that the susceptibility of a protein to cotranslational *N*-myristoylation could easily be detected by metabolic labeling in an in vitro or in vivo expression system using a fusion protein in which the N-terminal sequence (~10 amino acid residues) of the query protein was fused to a model protein [9]. In the present study, we utilized this strategy to detect posttranslational *N*-myristoylation of caspase substrates. In this case, the initiating Met was inserted at the N-terminus of the newly exposed N-terminus of the caspase-cleavage products and the susceptibility of the N-terminal sequence to protein *N*-myristoylation was evaluated by the same methods as described above. As a result, it was found that the N-terminal nine residues of the newly exposed N-terminus of the caspase-cleavage products of cytoskeletal actin and gelsolin efficiently direct the protein *N*-myristoylation. In fact, when COS-1 cells transiently transfected with cDNA coding for epitope-tagged actin were treated with staurosporine, an apoptosis-inducing agent, an *N*-myristoylated truncated actin (tActin) was generated as demonstrated by in vivo metabolic labeling with [^{3}H]myristic acid. Immunofluorescence staining coupled with MitoTracker or fluorescence tagged-phalloidin staining revealed that exogenously expressed tActin colocalized with mitochondria without affecting cellular and actin morphology. These results clearly dem-

*Corresponding author. Fax: (81)-83-933 5820.
E-mail address: utsumi@agr.yamaguchi-u.ac.jp (T. Utsumi).

Abbreviations: tBID, truncated BID; tActin, truncated actin; TNF, tumor necrosis factor; NMT, *N*-myristoyltransferase; PCR, polymerase chain reaction; DPBS, Dulbecco's phosphate-buffered saline; SDS, sodium dodecyl sulfate; PAGE, polyacrylamide gel electrophoresis

0014-5793/03/$22.00
doi:10.1016/S0014-5793(03)00180-7

onstrated that the C-terminal 15 kDa fragment of cytoskeletal actin is posttranslationally *N*-myristoylated upon caspase-mediated cleavage during apoptosis and targeted to mitochondria. Thus, the metabolic labeling of a fusion protein having a newly exposed N-terminus is a useful strategy to detect post-translational *N*-myristoylation of cellular proteins. This is the first report, to our knowledge, showing that posttranslational *N*-myristoylation occurred on other caspase substrates as well as on a pro-apoptotic protein BID.

2. Materials and methods

2.1. Materials

Restriction endonucleases, DNA-modifying enzymes, RNase inhibitor, and Taq DNA polymerase were purchased from Takara Shuzo, Kyoto, Japan. RNase was obtained from Boehringer-Mannheim, Germany. [^{3}H]leucine, [^{3}H]myristic acid, and Amplify were from Amersham, UK. The Dye Terminator Cycle Sequencing kit was from Applied Biosystems, USA. Anti-human tumor necrosis factor (TNF) polyclonal antibody was purchased from R&D systems, USA. Anti-FLAG monoclonal antibody and TRITC-conjugated phalloidin were purchased from Sigma, USA. MitoTracker red CM-H_2XRos was obtained from Molecular Probes, The Netherlands. Protein G Sepharose was from Pharmacia Biotech, Sweden. Plasmid pEYFP-Actin was obtained from Clontech, USA. Other reagents purchased from Wako Pure Chemical, Daiichi Pure Chemicals, and Seikagaku Kogyo (Japan) were of analytical or DNA grade.

2.2. Plasmid construction

Plasmid pBluescript II SK(+) lacking *Apa*I and *Hin*DIII sites was constructed as previously described [10], and designated pB. Plasmid pBΔpro-TNF, which contains a cDNA coding for the mature domain of TNF, was constructed as described in [11,12]. Plasmid pBtBID-TNF was constructed by utilizing polymerase chain reaction (PCR). For this procedure, pBΔpro-TNF served as a template and two oligonucleotides (tBID, B1) served as primers (Table 1). After digestion with *Bam*HI and *Pst*I, the amplified product was subcloned into pB at *Bam*HI and *Pst*I sites. Plasmids pBtPARP-, pBtPKCζ-, pBtp59^{FYN}-, pBtActin-, pBtGelsolin- and pBtMEKK-1-TNF were constructed by a method similar to that of pBtBID-TNF using two oligonucleotides (tPARP plus B1, tPKCζ plus B1, tp59^{FYN} plus B1, tActin plus B1, tGelsolin plus B1 and tMEKK-1 plus B1, respectively) as primers (Table 1). Plasmid pB-FLAG, which contains the sequence for the FLAG epitope at the C-terminus, was constructed as follows. The *Eco*RI/*Apa*I fragment coding for FLAG epitope was excised from PCMV-Tag4 vector (Stratagene) and then subcloned into pBluescript II SK(+) at *Eco*RI and *Apa*I sites. Plasmid pBtActin-FLAG, which contains a cDNA coding for FLAG-tagged tActin, was constructed by utilizing PCR. For this procedure, pEYFP-Actin (Clontech) served as a template and two oligonucleotides (N-ACT15, C-ACT) as primers (Table 1). After digestion with *Bam*HI and *Eco*RI, the amplified product was subcloned into pB-FLAG at *Bam*HI and *Eco*RI sites. Plasmid pBtActinG2A-FLAG was constructed by a method similar to that of pBtActin-FLAG using two oligonucleotides (tACTG2A, C-ACT) as primers (Table 1). Plasmid pBActin-FLAG, which contains a cDNA coding for FLAG-tagged full-length actin, was constructed by a method similar to that of pBtActin-FLAG using two oligonucleotides (N-ACT, C-ACT) as primers (Table 1). The DNA sequences of these recombinant cDNAs were confirmed by the dideoxy-nucleotide chain termination method [13]. The cDNAs coding for TNF mutants and actin mutants were subcloned into pcDNA3 and the obtained pcDNA3 constructs were used for transfection assay.

2.3. Transfection of COS-1 cells and determination of N-myristoylated proteins

The simian virus 40-transformed African Green monkey kidney cell line, COS-1, was maintained in Dulbecco's modified Eagle's medium (DMEM; Gibco BRL) supplemented with 10% fetal calf serum (FCS; Gibco BRL). Cells (2×10^5) were plated onto 35 mm diameter dishes 1 day before transfection. pcDNA3 construct (2 μg; Invitrogen, San Diego, CA, USA) containing cDNA coding for mutant TNF or actin was used to transfect each plate of COS-1 cells along with 4 μl of LipofectAmine (2 mg/ml; Gibco BRL) in 1 ml of serum-free medium. After incubation for 5 h at 37°C, the cells were refed with serum-containing medium and incubated again at 37°C for 48 h. The cells were then washed twice with 1 ml of serum-free DMEM and incubated for 5 h at 37°C in 1 ml of DMEM with 2% FCS containing [^{3}H]myristic acid (100 μCi/ml). For the treatment with staurosporine, the cells were first incubated at 37°C for 2 h in 1 ml of DMEM with 2% FCS containing [^{3}H]myristic acid (100 μCi/ml). Staurosporine was added to the medium at a final concentration of 2 μM, and then the cells were further incubated at 37°C for 4 h. Subsequently, the cells were washed three times with Dulbecco's phosphate-buffered saline (DPBS) and collected with cell scrapers, followed by lysis with 200 μl of RIPA buffer [50 mM Tris–HCl (pH 7.5), 150 mM NaCl, 1% Nonidet P-40, 0.5% sodium deoxycholate, 0.1% sodium dodecyl sulfate (SDS), proteinase inhibitors] on ice for 20 min. After immunoprecipitation with anti-TNF or anti-FLAG antibody, the samples were analyzed by SDS–PAGE (polyacrylamide gel electrophoresis) and fluorography.

2.4. Western blotting

The total cell lysates of each group of transfected cells were obtained at 48 h after transfection and resolved by 12.5% SDS–PAGE and then transferred to an Immobilon-P transfer membrane (Millipore). After blocking with non-fat milk, the membrane was probed with a specific anti-TNF or anti-FLAG antibody as described previously [14]. Immunoreactive proteins were specifically detected by incubation with horseradish peroxidase-conjugated Protein G (Bio-Rad). The membrane was developed with enhanced chemiluminescence Western blotting reagent (Amersham) and exposed to X-ray film (Kodak).

2.5. Immunoprecipitation

Samples were immunoprecipitated with a specific anti-TNF or anti-FLAG antibody as described in [10].

2.6. SDS–PAGE and fluorography

Samples were denatured by boiling for 3 min in SDS-sample buffer followed by analysis by SDS–PAGE on a 12.5% gel. Thereafter, the gel was fixed and soaked in Amplify™ (Amersham) for 20 min. The gel was dried under vacuum and exposed to X-ray film (Kodak) for an appropriate period.

2.7. Immunofluorescence analysis and fluorescence microscopy

Immunofluorescence analysis of transfected cells was performed at 48 h after transfection. At this time point, the maximum level of protein expression was achieved. For immunocytochemistry, cells were washed with DPBS, fixed in 4% paraformaldehyde in DPBS for 15 min, and permeabilized with 0.1% Triton X-100 in DPBS for 10 min at room temperature, followed by washing with 0.1% gelatin in DPBS. The permeabilized cells were incubated with anti-FLAG antibody (1:1000) in DPBS for 1 h at room temperature. After washing with 0.1% gelatin in DPBS, the cells were incubated with FITC-conjugated anti-mouse IgG antibody for 1 h at room temperature. Mitochondria were identified with 300 nM MitoTracker red, which was incubated with the cells for 30 min before fixation. To observe filamentous actin, the fixed and permeabilized cells were incubated with 40 nM TRITC-conjugated phalloidin for 45 min at room temperature. After washing with 0.1% gelatin in DPBS, the cells were observed under a Zeiss Axiovert microscope.

3. Results

3.1. N-terminal sequence of the newly exposed N-terminus of tActin and tGelsolin efficiently directs protein N-myristoylation

To determine whether the N-terminal sequence of the newly exposed N-terminus of the truncated BID (tBID) could direct cotranslational protein *N*-myristoylation, N-terminal nine residues of the mature domain of TNF were replaced with those of tBID to generate tBID-TNF (Fig. 1). In this case, the initiating Met was inserted at the N-terminus of the fusion protein. Then, its susceptibility to protein *N*-myristoylation

Table 1
Nucleotide sequences of oligonucleotides used for the plasmid construction

Primer	Sequence
tBID	5′-GCGCGGATCCATGGGCAACCGCAGCAGCCACTCCCGCTTGGACAAGCCTGTAGCC-3′
tPARP	GCGCGGATCCATGGGAGTGGATGAAGTGGCGAAGAAGAAAGACAAGCCTGTAGCC
tp59^{FYN}	GCGCGGATCCATGGGCAGCCTGAACCAGAGCTCTGGGTACGACAAGCCTGTAGCC
tPKCζ	GCGCGGATCCATGGGAATCAAAATCTCTCAGGGGCTTGGGGACAAGCCTGATGCC
tActin	GCGCGGATCCATGGGCCAGGTCATCACCATTGGCAATGAGGACAAGCCTGTAGCC
tGelsolin	GCGCGGATCCATGGGCCTGGGCTTGTCCTACCTTTCCAGCGACAAGCCTGTAGCC
tMEKK-1	GCGCGGATCCATGGGTCAACAGGACAGCTTCTTGCAGGCAGACAAGCCTGTAGCC
B1	GCCGGGATCCTAGGGCGAATTGGGTACC
T3	AATTAACCCTCACTAAAGGG
N-ACT	GCGCGGATCCATGGATGATGATATC
N-ACT15	ATATGGATCCATGGGCCAGGTCATCACC
tACTG2A	ATATGGATCCATGGCCCAGGTCATCACC
C-ACT	GCGCGAATTCGAAGCATTTGCGGTG
ECO-FLAG	GCGCGAATTCCAGGGCAATGATCCC

was evaluated by in vivo metabolic labeling in transfected cells.

When tBID-TNF was expressed in COS-1 cells, efficient expression of a protein with an expected molecular mass (17 kDa) was observed as determined by Western blotting using anti-TNF antibody as shown in Fig. 2A, lane 1. Metabolic labeling with [^{3}H]myristic acid revealed an efficient incorporation of [^{3}H]myristic acid into tBID-TNF (Fig. 2B, lane 1).

To search for caspase substrates that would be posttranslationally *N*-myristolyated upon caspase-mediated cleavage, the susceptibility of the N-terminal sequence of the newly exposed N-terminus of several caspase substrates to protein *N*-myristoylation was evaluated by in vivo metabolic labeling using the strategy described above. In this case, six caspase substrates (PARP, PKCζ, p59^{FYN}, actin, gelsolin, and MEKK-1) that expose an N-terminal Gly upon cleavage were selected as possible candidates. As shown in Fig. 2A, efficient protein expression was observed with tPARP-, tPKCζ-, tp59^{FYN}-, tActin-, tGelsolin-, and tMEKK-1-TNF as with tBID-TNF, as determined by Western blotting. [^{3}H]myristic acid labeling revealed that tActin- and tGelsolin-TNF were efficiently *N*-myristoylated as was tBID-TNF (Fig. 2B, lanes 5 and 6). The efficiency of [^{3}H]myristic acid incorporation into tActin- and tGelsolin-TNF was comparable to that into tBID-TNF.

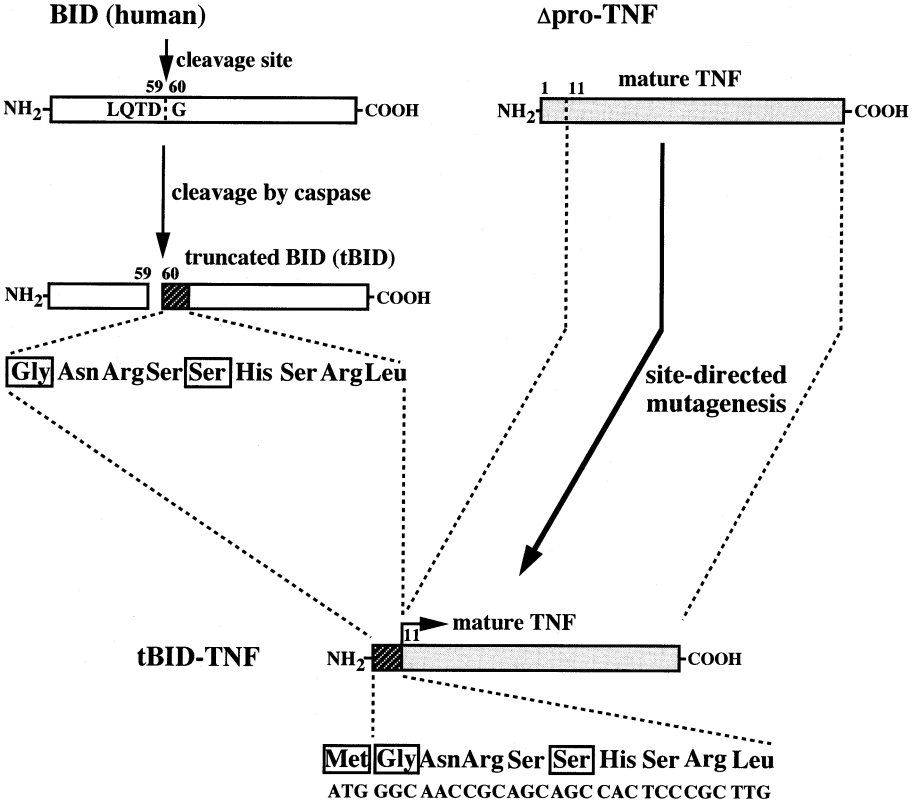

Fig. 1. Schematic representation of the generation of tBID-TNF. The cDNA coding for tBID-TNF was generated from Δpro-TNF cDNA by site-directed mutagenesis. The N-terminal nine residues of the mature domain of TNF were replaced with those of tBID and the initiating Met was introduced at the N-terminus to generate tBID-TNF.

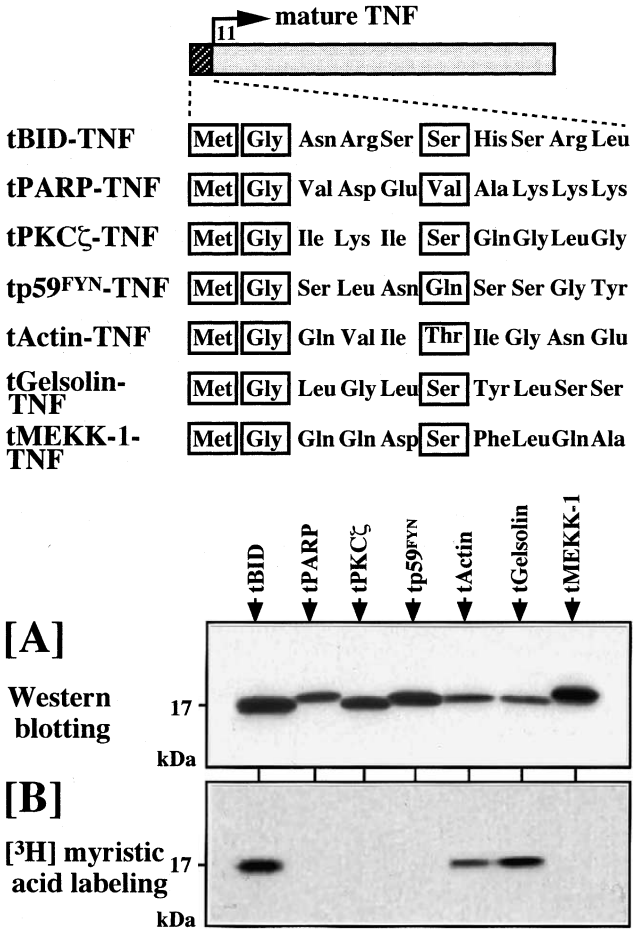

Fig. 2. N-terminal sequence of the newly exposed N-terminus of tActin and tGelsolin efficiently directs protein *N*-myristoylation. tBID-, tPARP-, tPKCζ-, tp59^{FYN}-, tActin-, tGelsolin-, and tMEKK-1-TNF were expressed in COS-1 cells and the cells were labeled with [^{3}H]myristic acid. A: Total cell lysates were analyzed by Western blotting using anti-TNF antibody. B: Following immunoprecipitation with anti-TNF antibody, the labeled proteins were analyzed by SDS–PAGE and fluorography.

In contrast, no incorporation of [^{3}H]myristic acid was observed with tPARP-, tPKCζ-, tp59^{FYN}-, and tMEKK-1-TNF despite the efficient expression of these proteins.

3.2. *In vivo expressed full-length tActin is efficiently N-myristoylated*

As shown in Table 2, the N-terminal sequence of the newly exposed N-terminus of tActin is highly conserved among various species, suggesting a critical role of the posttranslational *N*-myristoylation of tActin in the physiology of cytoskeletal actin. In contrast, the N-terminal sequence of the newly exposed N-terminus of tGelsolin is not conserved. Since Pro at the amino acid at position 3 has been shown to inhibit protein *N*-myristoylation, it is quite probable that posttranslational *N*-myristoylation will not occur on pig- and mouse-tGelsolin. Therefore, we chose actin to further analyze the posttranslational *N*-myristoylation of protein.

To confirm that the full-length tActin is *N*-myristoylated, cDNAs coding for epitope-tagged actin and tActin were generated and their susceptibility to protein *N*-myristoylation was evaluated by in vivo metabolic labeling. In this case, a FLAG-tag was introduced at the C-terminus of these constructs. As shown in Fig. 3A, lane 3, transfection of COS-1 cells with cDNA coding for FLAG-tagged tActin gave rise to a 17 kDa protein band with an expected molecular mass (15 kDa tActin plus 2 kDa linker and FLAG-tag). The 17 kDa protein band was efficiently *N*-myristoylated as determined by [^{3}H]myristic acid labeling (Fig. 3B, lane 3). When Gly2 of tActin-FLAG was replaced with Ala (tActinG2A-FLAG), [^{3}H]myristic acid incorporation was completely inhibited, as shown in Fig. 3A,B, lane 4. Interestingly, transfection of FLAG-tagged actin gave rise to two protein bands; one is a non-myristoylated major band with an expected molecular mass (47 kDa: 45 kDa actin plus 2 kDa linker and FLAG-tag) and the other is a fainter *N*-myristoylated 17 kDa protein band (Fig. 3A,B, lane 1). These results indicated that actin could be intracellularly cleaved to generate *N*-myristoylated tActin.

3.3. *Induction of apoptosis enhances the generation of N-myristoylated tActin*

To determine whether the intracellular generation of *N*-myristoylated tActin is induced by caspase-mediated cleavage of actin during apoptosis, COS-1 cells transfected with FLAG-tagged actin were treated with staurosporine, an inducer of apoptosis, and the generation of *N*-myristoylated tActin was determined by Western blotting and [^{3}H]myristic acid labeling. When COS-1 cells were treated with 2 μM staurosporine, the cells died with the typical feature of apoptosis. As shown in Fig. 4A,B, lanes 3 and 4, the amount of *N*-myristoylated tActin was increased by the treatment with staurosporine. This enhancement was significantly inhibited when cells were pretreated with 100 μM of Z-VAD-fmk, a caspase inhibitor, before addition of staurosporine (Fig. 4A,B, lane 5). These results strongly indicated that the generation of *N*-myristoylated tActin is induced by caspase-mediated cleavage of actin during apoptosis.

Table 2
Comparison of the amino acid sequence around the caspase-cleavage site of actin and gelsolin derived from various species

	Substrate	Sequence
β-Actin	human	SLEKSYELPD ↓ **G** QVI TIGNERFRCPEALFQP
	pig	SLEKSYELPD ↓ **G** QVI TIGNERFRCPEALFQP
	horse	SLEKSYELPD ↓ **G** QVI TIGNERFRCPEALFQP
	mouse	SLEKSYELPD ↓ **G** QVI TIGNERFRCPEALFQP
	rat	SLEKSYELPD ↓ **G** QVI TIGNERFRCPEALFQP
	monkey	SLEKSYELPD ↓ **G** QVI TIGNERFRCPEALFQP
Gelsolin	human	KNWRDPDQTD ↓ **G** LGL SYLSSHIANVERVPFD
	pig	KNWRDPDQVD ↓ **G** PGL SYLSSHIANVERVPFD
	horse	KNWRDPDQTE ↓ **G** LGL AYLSSHIAHVERVPFD
	mouse	KNWRDPDQTD ↓ **G** PGL GYLSSHIANVERVPFD

Caspase-cleavage sites are indicated by arrows. The N-terminal Gly at the newly exposed N-terminus is represented in bold-face.

3.4. *Exogenously expressed tActin colocalized with mitochondria without affecting cellular and actin morphology*

When exogenously expressed in COS-1 cells, Actin-FLAG colocalized with cellular filamentous actin as determined by the immunofluorescence staining coupled with fluorescence tagged-phalloidin staining as shown in the upper panels of Fig. 5. In contrast, exogenously expressed tActin-FLAG did not colocalize with filamentous actin but showed clustered localization within the cell without affecting cellular and actin morphology, as shown in the lower panels of Fig. 5.

Immunofluorescence staining coupled with MitoTracker staining revealed colocalization of tActin-FLAG with mitochondria, as shown in the upper panels of Fig. 6. The fact that tActinG2A-FLAG showed diffuse cytosolic distribution indicated that *N*-myristoylation of tActin promotes its targeting to mitochondria (lower panel of Fig. 6). As in the case of tActin-FLAG expression, expression of tActinG2A-FLAG did not affect cellular and actin morphology (data not shown).

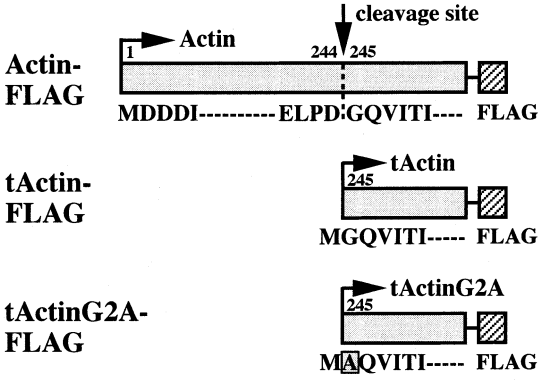

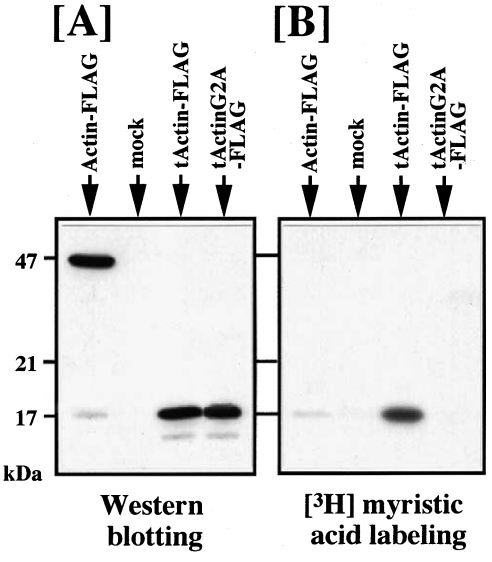

Fig. 3. tActin expressed in COS-1 cells is efficiently *N*-myristoylated. Actin-FLAG, tActin-FLAG and tActinG2A-FLAG were expressed in COS-1 cells and the cells were labeled with [^{3}H]myristic acid. A: Total cell lysates were analyzed by Western blotting using anti-FLAG antibody. B: Following immunoprecipitation with anti-FLAG antibody, the labeled proteins were analyzed by SDS–PAGE and fluorography.

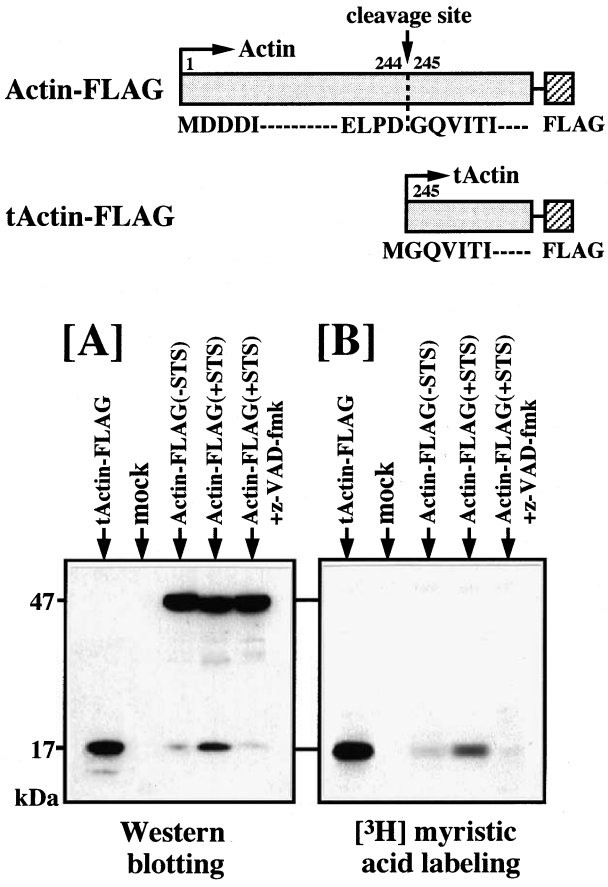

Fig. 4. Induction of apoptosis enhances the generation of *N*-myristoylated tActin. COS-1 cells transfected with cDNA coding for Actin-FLAG were first incubated at 37°C for 2 h in 1 ml of DMEM with 2% FCS containing [^{3}H]myristic acid (100 μCi/ml). Staurosporine was added to the medium at a final concentration of 2 μM, then the cells were further incubated at 37°C for 4 h. For the treatment of z-VAD-fmk, the cells were pretreated with 100 μM of z-VAD-fmk for 2 h before addition of staurosporine. A: Total cell lysates were analyzed by Western blotting using anti-FLAG antibody. B: Following immunoprecipitation with anti-FLAG antibody, the labeled proteins were analyzed by SDS–PAGE and fluorography.

4. Discussion

Protein *N*-myristoylation has long been recognized as a cotranslational protein modification. Recently, it was demonstrated that *N*-myristoylation can also occur posttranslationally, as in the case of pro-apoptotic protein BID [7]. This post-proteolytic *N*-myristoylation of BID was found to promote its targeting to mitochondria as well as to enhance its pro-apoptotic action in vivo. Since 16 of ~60 identified caspase substrates listed in a recent review [8] expose an N-terminal Gly upon cleavage, it was suggested that the posttranslational *N*-myristoylation might be a common modification in apoptosis and perhaps other proteolytic pathways [7]. However, so far, BID is the only protein that has been proved to be posttranslationally *N*-myristoylated upon caspase-mediated cleavage. In the present study, we tried to search for caspase substrates that are posttranslationally *N*-myristoylated upon caspase-mediated cleavage. As it was demonstrated that NMT, the enzyme responsible for cotranslational *N*-myristoylation, could catalyze posttranslational *N*-myristoylation of

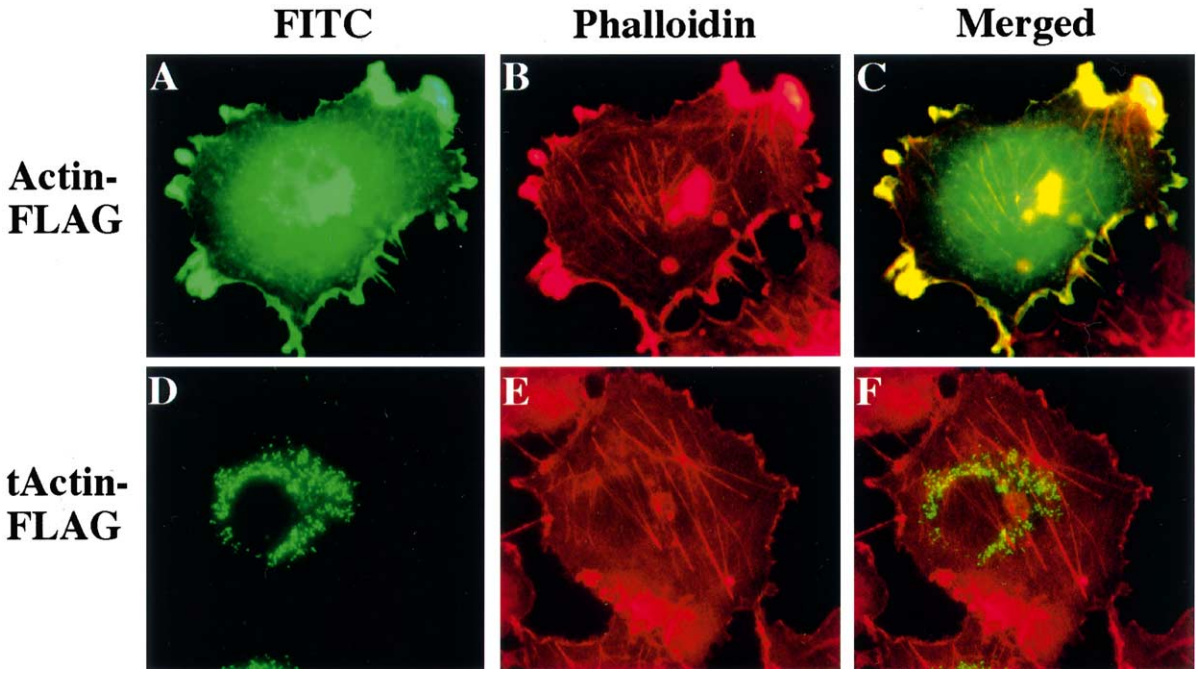

Fig. 5. Exogenously expressed tActin did not affect cellular or actin morphology. A,D: Subcellular localization of Actin-FLAG (panel A) and tActin-FLAG (panel D) expressed in COS-1 cells was determined by immunofluorescence staining using anti-FLAG antibody. B,E: Filamentous actin in these cells was observed by TRITC-conjugated phalloidin staining. C,F: The merged image is shown.

BID, it is quite probable that the enzyme responsible for posttranslational *N*-myristoylation is NMT.

NMT has been purified and cloned from several organisms [15–18]. The precise substrate specificity of this enzyme has been characterized using purified enzyme and synthetic peptide substrates [2,19,20]. In general, Ser or Thr is preferred at position 6 and the N-terminal consensus motifs such as Met-Gly-X-X-X-Ser/Thr-X-X [21] or Met-Gly-X-X-X-Ser/Thr-X-X-X [5] that direct protein *N*-myristoylation have been defined. However, Ser or Thr at position 6 is neither sufficient

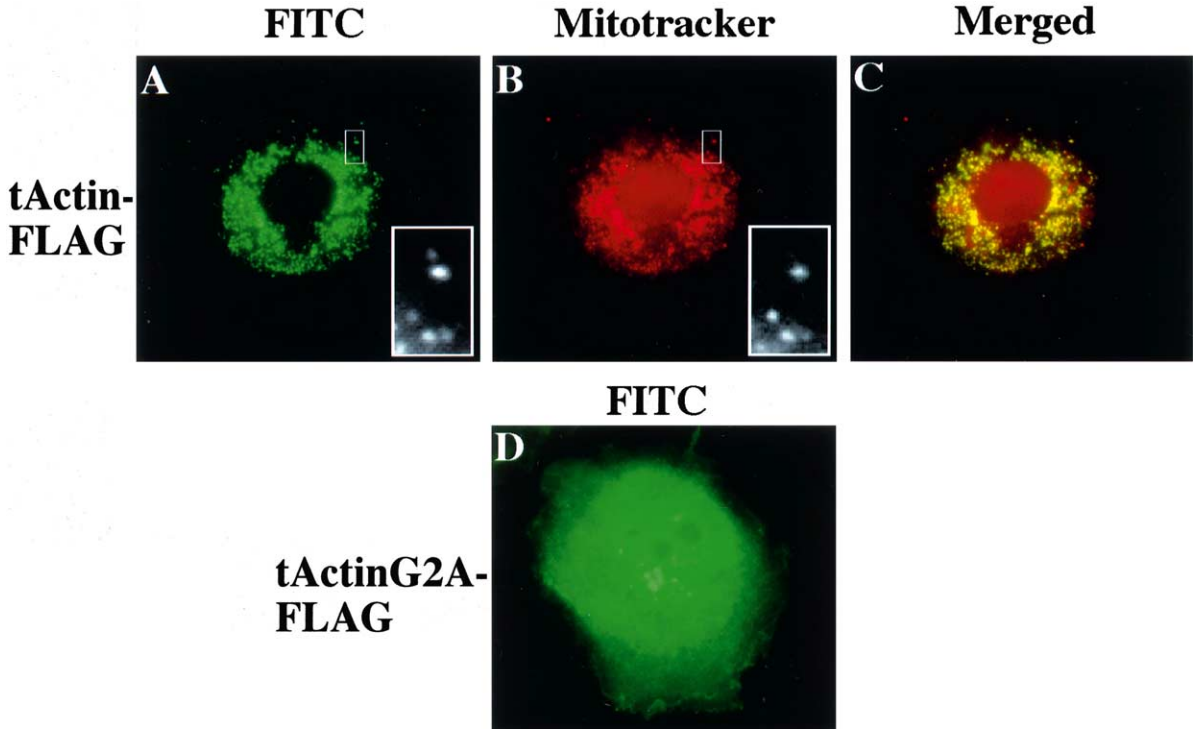

Fig. 6. Colocalization of exogenously expressed tActin with mitochondria. A,D: Subcellular localization of tActin-FLAG (panel A) and tActin-G2A-FLAG (panel D) expressed in COS-1 cells was determined by immunofluorescence staining using anti-FLAG antibody. B: Mitochondria in the same cell in panel A were identified by MitoTracker staining. C: The merged image is shown. Black and white image in panels A and B shows the close-up (×4) view of the area surrounded by white box.

nor critical for the recognition of the protein substrate by the NMT. Some amino acid preferences were also reported at other positions such as 3, 7 and 8 [2,22]. Recently, a sophisticated program for automated prediction of protein *N*-myristoylation from the substrate protein sequence has been developed and this prediction program is available as public WWW-server [23,24]. When 16 caspase substrates having an internal Gly residue that becomes an N-terminus after cleavage by caspase were investigated using this prediction program, a 'reliable' myristoylation site was predicted only with BID.

Previously, we have shown that the susceptibility of a protein to cotranslational *N*-myristoylation could easily be detected by metabolic labeling in an in vitro or in vivo expression system using a fusion protein in which the N-terminal sequence (~10 amino acid residues) of the query protein was fused to a model protein [9]. With this experimental procedure, we found that the amino acid residue penultimate to the N-terminal Gly residue strongly affects two cotranslational protein modifications, *N*-myristoylation and *N*-acetylation [9]. In the present study, we utilized this strategy to detect posttranslational *N*-myristoylation of caspase substrates.

As a result, it was found that the N-terminal nine residues of the newly exposed N-terminus of the caspase-cleavage products of cytoskeletal actin and gelsolin efficiently direct the protein *N*-myristoylation. In fact, when COS-1 cells transiently transfected with cDNA coding for epitope-tagged full-length actin were treated with staurosporine, an apoptosis-inducing agent, an *N*-myristoylated tActin was generated, as demonstrated by in vivo metabolic labeling with [^{3}H]myristic acid. Immunofluorescence staining coupled with MitoTracker or fluorescence tagged-phalloidin staining revealed that exogenously expressed tActin colocalized with mitochondria without affecting cellular and actin morphology.

Apoptosis accompanies a dramatic reorganization of the cytoskeleton, which is followed by morphological changes and cellular fragmentation. The involvement of the actin filament in the morphological changes of apoptosis has been suggested by some inhibitor studies [25]. It was found that actin is the substrate of caspases [26,27] and actin fragments cleaved by caspase-1 could not polymerize effectively in vitro [28]. Recently, it was reported by Mashima et al. that, in some tumor cells, induction of apoptosis was accompanied by caspase-dependent actin-cleavage to 31 and 15 kDa fragments [29]. It was also found that ectopic expression of the 15 kDa C-terminal fragment, but not the 31 kDa N-terminal fragment, induced morphological changes resembling those of apoptotic cells, while the 15 kDa fragment expression caused neither caspase activation nor cleavage of a marker substrate protein, PARP. Thus, generation of tActin seems to play a positive role in the morphological changes of apoptosis downstream of caspase activation. In the present study, however, it was clearly demonstrated from fluorescence tagged-phalloidin staining that exogenously expressed tActin did not affect cellular or actin morphology. These results form a striking contrast to the results obtained by Mashima et al. One possible explanation for the discrepancy might be the difference in the cell line used for the analysis. To test this possibility, the same experiments reported in the present study were performed using 293T cells used in the study by Mashima et al. and the obtained results were compared with those of COS-1 cells. As a result, the same level of protein expression and [^{3}H]myristic acid incorporation was observed when tActin was expressed in these two cell lines (data not shown). In addition, similar subcellular localization of tActin was observed and no obvious changes in overall cell morphology or the actin cytoskeleton were detected. Therefore, the difference in the cell line used for the study is not the reason for the discrepancy. Thus, we could not obtain the experimental evidence that explains the obvious discrepancy between our data and those of Mashima et al.

Instead of affecting actin structure, tActin was found to colocalize with mitochondria. The fact that replacement of Gly2 of tActin with Ala completely inhibited its localization to mitochondria indicated that *N*-myristoylation of tActin promotes its targeting to mitochondria. In the case of tBID, *N*-myristoylation is directly involved in BID targeting to mitochondria, its insertion into the outer membrane of mitochondria, the release of cytochrome c, and the killing of cells. In contrast, tActin localized at mitochondria did not induce cellular apoptosis. Further studies are required to reveal the physiological roles of mitochondrial localization of tActin.

Another important issue to be clarified is the mechanism for mitochondrial targeting of tActin. Recent studies using GFP chimeras containing *N*-myristoylation signal revealed that *N*-myristoylated chimeric GFPs were localized to intracellular membranes including endoplasmic reticulum and endosomes, and were absent from mitochondria [30]. The fact that both of the posttranslationally *N*-myristoylated proteins so far discovered localized to mitochondria but not to other intracellular membranes might indicate that posttranslational protein *N*-myristoylation functions as a novel form of mitochondrial targeting signal. Further analyses are required to clarify the molecular mechanisms for mitochondrial targeting of these proteins.

Acknowledgements: We thank Dr. Mitsuaki Tabuchi for helpful technical suggestions. Part of this work was supported by a Grant-in-Aid for Scientific Research (No. 12660080) from the Ministry of Education, Science and Culture of Japan.

References

[1] Sefton, B.M. and Buss, J.E. (1987) J. Cell Biol. 104, 1449–1453.
[2] Towler, D.A., Gordon, J.I., Adams, S.P. and Glaser, L. (1988) Annu. Rev. Biochem. 57, 69–99.
[3] Spiegel, A.M., Backlund, P.S., Butrynski, J.E., Jones, T.L.Z. and Simonds, W.F. (1991) Trends Biochem. Sci. 16, 338–341.
[4] Wedegaertner, P.B., Wilson, P.T. and Bourne, H.R. (1995) J. Biol. Chem. 270, 503–506.
[5] Boutin, J.A. (1997) Cell Signal 9, 15–35.
[6] Resh, M.D. (1999) Biochem. Biophys. Acta 1451, 1–16.
[7] Zha, J., Weiler, S., Oh, K.-J., Wei, M.C. and Korsmeyer, S.J. (2000) Science 290, 1761–1765.
[8] Nicholson, D.W. (1999) Cell Death Differ. 6, 1028–1042.
[9] Utsumi, T., Sato, M., Nakano, K., Takemura, D., Iwata, H. and Ishisaka, R. (2001) J. Biol. Chem. 276, 10505–10513.
[10] Utsumi, T., Akimaru, K., Kawabata, Z., Levitan, A., Tokunaga, T., Tang, P., Ide, A., Hung, M.-C. and Klostergaard, J. (1995) Mol. Cell. Biol. 15, 6398–6405.
[11] Utsumi, T., Kuranami, J., Tou, E., Ide, A., Akimaru, K., Hung, M.-C. and Klostergaard, J. (1996) Arch. Biochem. Biophys. 326, 179–184.
[12] Utsumi, T., Tou, E., Takemura, D., Ishisaka, R., Yabuki, M. and Iwata, H. (1998) Arch. Biochem. Biophys. 349, 216–224.
[13] Sanger, F., Nicklen, S. and Collson, A.R. (1977) Proc. Natl. Acad. Sci. USA 74, 5463–5467.
[14] Utsumi, T., Takeshige, T., Tanaka, K., Takami, K., Kira, Y., Klostergaard, J. and Ishisaka, R. (2001) FEBS Lett. 500, 1–6.

[15] Towler, D.A., Adams, S.P., Eubanks, S.R., Towery, D.S., Jackson-Machelski, E., Glaser, L. and Gordon, J.I. (1987) Proc. Natl. Acad. Sci. USA 84, 2706–2712.
[16] Duronio, R.J., Reed, S.I. and Gordon, J.I. (1992) Proc. Natl. Acad. Sci. USA 89, 4129–4133.
[17] Lodge, J.K., Johnson, R.L., Weinberg, R.A. and Gordon, J.I. (1994) J. Biol. Chem. 269, 2996–3009.
[18] Giang, D.K. and Cravatt, B.F. (1998) J. Biol. Chem. 273, 6595–6598.
[19] Towler, D.A., Adams, S.P., Eubanks, S.R., Towery, D.S., Jackson-Machelski, E., Glaser, L. and Gordon, J.I. (1988) J. Biol. Chem. 263, 1784–1790.
[20] Rocque, W.J., McWherter, C.A., Wood, D.C. and Gordon, J.I. (1993) J. Biol. Chem. 268, 9964–9971.
[21] Johnson, D.R., Bhatnagar, R.S., Knoll, L.J. and Gordon, J.I. (1994) Annu. Rev. Biochem. 63, 869–914.
[22] McWherter, C.A., Rocque, W.J., Zupec, M.E., Freeman, S.K., Brown, D.L., Devadas, B., Getman, D.P., Sikorski, J.A. and Gordon, J.I. (1997) J. Biol. Chem. 272, 11874–11880.
[23] Maurer-Stroh, S., Eisenhaber, B. and Eisenhaber, F. (2002) J. Mol. Biol. 317, 523–540.
[24] Maurer-Stroh, S., Eisenhaber, B. and Eisenhaber, F. (2002) J. Mol. Biol. 317, 541–557.
[25] Cotter, T.G., Lennon, S.V., Glynn, J.M. and Green, D.R. (1992) Cancer Res. 52, 997–1005.
[26] Mashima, T., Naito, M., Fujita, N., Noguchi, K. and Tsuruo, T. (1995) Biochem. Biophys. Res. Commun. 217, 1185–1192.
[27] Mashima, T., Naito, M., Noguchi, K., Miller, D.K., Nicholson, D.W. and Tsuruo, T. (1997) Oncogene 14, 1007–1012.
[28] Kayalar, C., Ord, T., Testa, M., Zhong, L.T. and Bredesen, D.E. (1996) Proc. Natl. Acad. Sci. USA 93, 2234–2238.
[29] Mashima, T., Naito, M. and Tsuruo, T. (1999) Oncogene 18, 2423–2430.
[30] McCabe, J.B. and Berthiaume, L.G. (1999) Mol. Biol. Cell 10, 3771–3786.